

Phosphoric Acid Based Geopolymer as a Novel Photocatalyst for Methylene Blue Dye Degradation in Wastewater

H. Majdoubi^{1*}, Y. Chraibi¹, Y. Haddaji², M. Nadi², R.E. Kaim Billah³, S. Sbi¹, M. Slimane^{1,2,4}, A. Soulaïmani², H. Hannache¹ and Y. Tamraoui¹

¹Mohamed VI Polytechnic University, Materials Science and Nanoengineering Department, Benguerir, Morocco

²Laboratory of engineering and materials LIMAT, Faculty of science Ben M'Sik, Hassan II University, Casablanca, Morocco

³Department of Chemistry, Faculty of Sciences, Laboratory of Coordination and Analytical Chemistry, University of Chouaib Doukkali, El Jadida, Morocco

⁴OCF Group

*Correspondence to:

H. Majdoubi

Mohamed VI Polytechnic University,
Materials Science and Nanoengineering Department,
Benguerir, Morocco.

E-mail: hichammajdoubi.hm@gmail.com;
hicham.majdoubi@um6p.ma

Received: July 25, 2023

Accepted: September 25, 2023

Published: September 28, 2023

Citation: Majdoubi H, Chraibi Y, Haddaji Y, Nadi M, Billah REK, et al. 2023. Phosphoric Acid Based Geopolymer as a Novel Photocatalyst for the Degradation of the Methylene Blue Dye in Wastewater. *NanoWorld J* 9(S2): S206-S213.

Copyright: © 2023 Majdoubi et al. This is an Open Access article distributed under the terms of the Creative Commons Attribution 4.0 International License (CCBY) (<http://creativecommons.org/licenses/by/4.0/>) which permits commercial use, including reproduction, adaptation, and distribution of the article provided the original author and source are credited.

Published by United Scientific Group

Abstract

This study presents a new application of phosphoric acid-based geopolymers and phosphate washing sludge (PW) as a photocatalyst for the degradation of methylene blue (MB) dye in wastewater. The aim of this work is to study the photodegradation of MB dye using PW@Geopolymer, exploring the effects of physico-chemical parameters such as initial pH and dye concentration on degradation kinetics. The kinetics of MB dye degradation are analyzed using pseudo-first and pseudo-second order rate equations, taking into account UV irradiation and non-irradiation conditions. The PW@Geopolymer photocatalyst exhibits high efficiency, achieving up to 91.7% MB dye degradation under UV irradiation. This performance is attributed to the combined effect of adsorption and semiconducting photocatalysis. The experimental data correlate closely with the pseudo-second order rate equation, indicating dominant adsorption kinetics. This research extends the applications of geopolymers by demonstrating their potential as efficient photocatalysts for MB dye removal from wastewater, providing valuable information on reaction kinetics, and highlighting the promising performance of PW@Geopolymer in eco-friendly dye degradation processes.

Keywords

Acid based geopolymer, Phosphate washing sludge, Photocatalysis, Degradation kinetics, Degradation efficiency

Introduction

The presence of dyes in water waste is considered a major environmental problem because of its impact on the environment and life. Due to increasing industrialization in the textile, paper, plastics, leather, processing, and furniture industries, the use of dyes is daily growing [1, 2]. In fact, about 700,000 tons of different types of dyes (nearly 100,000 types) are produced every day [3]. Moreover, watercolor is considered an important parameter for controlling water quality, as the presence of trace amounts of dyes is easily observed. Hence undesirable. Most dyes are large organic molecules. MB is one of the most used dyes in the textile and furniture industries. MB in water waste can lead to permanent blindness, asthma, and abdominal problems such as vomiting and nausea. Therefore, MB removal from wastewater is necessary for health and environmental reasons [2, 4]. Removal of colorants from wastewater can be achieved by adsorption, photodegradation, ultrafiltration, ion exchange, and electrochemical and non-chemical decomposition which is achieved by applying various methods such as reverse

osmosis [5]. The complexity of treatment protocols, high costs, and large volumes of contaminated water make water treatment scenarios more complicated, so looking for new, cheap, and simple materials and methods for wastewater treatment is essential [6]. Adsorption is considered one of the most effective wastewater treatment techniques due to the existence of several adsorbent materials that are cheap, readily available, and can be prepared using simple synthetic protocols. Many studies were made to search for alternative substances that can decontaminate wastewater [7]. MB for example is the most used sorbents for its removal include biosorbents, wood, rice husk ash, zeolites, fly ash, chitosan, cellulose, kapok, cotton, and geopolymers [8-10]. Although these materials have been successful in effectively removing colorants from wastewater, some issues remain to be addressed. In fact, adsorbent recycling and regeneration are of utmost importance as they contribute to the sustainability of the process. Additionally, another point to address is the thermal stability of the material. Most organic sorbents are difficult to recycle and reuse due to their thermal stability and solubility in organic solvents used for MB regeneration [1, 11].

The easy recyclability and thermal stability up to 1000 °C make geopolymers suitable adsorbents for wastewater treatment [12-16]. Geopolymers are environmentally friendly materials produced by the chemical interaction of raw aluminosilicate sources. Coal fly ash, calcined clay (Metakaolin; MK), metallurgical slag, silicate, or phosphoric acid in alkaline and aqueous solutions are used to accelerate the reaction process and produce a solid, insoluble binder material. Geopolymers were first introduced by Davidovits back in the 70s, it introduces alkali-activated MK which is marketed as a refractory inorganic material [17-21]. Furthermore, it offers interesting applications with diverse chemical, structural and zeolite-like properties such as thermal and corrosion stability and their physical properties [22-25]. Due to their inherent porosity, geopolymers are used as adsorbent materials and photocatalysts for the removal of metallic contaminants, organic dyes from water waste, and indoor formaldehyde adsorption [14, 26]. The adsorption capacity of alkali-activated materials is many times higher than that of the parent precursor [27, 28]. Recently, a new class of geopolymers was prepared by activating MK with phosphoric acid and named acidic geopolymers, provided interesting properties, thermal stability, and porosity. So, it may be a suitable alternative for wastewater treatment either as adsorption or photocatalysis materials. Reportedly, acidic geopolymers have important adsorption properties, which will make these polymers play an important role in wastewater treatment [4, 29]. Furthermore, with the advancements in scientific research on this particular class of geopolymers, numerous studies have demonstrated the potential for valorizing industrial by-products, particularly the waste generated by the phosphate industry. Multiple studies have highlighted the environmental and economic aspects of geopolymers derived from phosphate industry by-products [13, 19, 21, 30, 31]. To the best of our knowledge, no existing study has utilized geopolymers derived from phosphate industry by-products for the elimination of organic pollutants.

The aim of this work is to investigate the suitability of

acidic geopolymers based PW for wastewater treatment applications, focusing on acidic geopolymer synthesis and characterization, photocatalytic degradation of MB and its kinetics.

Experimentation

Materials and preparation

Kaolin clay, which is sold commercially, was employed as a source of aluminosilicates. In a muffle furnace, the kaolin clay was calcined at 750 °C for two hours to create reactive amorphous MK [31]. The PW utilized in this investigation was gathered from the Khouribga region's Moroccan phosphate purification industry. The data for raw materials are shown in table 1. To make the 10 mol/L acid activating solution, 85 weight percent of commercial phosphoric acid (H_3PO_4) was diluted in distilled water. The selection of this concentration was based on earlier publications in the literature [32], where it was said that this concentration was most suited for making acidic geopolymers. The following mixing and curing procedures were used in the preparation of PW@Geopolymer: To create solid precursors (MK + PG), PW powder was first mixed with MK at a ratio of MK/PW = 1, which was then added to the 10 mol/L of H_3PO_4 solution at a H_3PO_4 /MK = 1 ratio. The PW@Geopolymer pastes that had been made were put into cube-shaped plastic molds. The molds go through a two-stage hardening process, the first of which lasts 24 hours at room temperature and the second of which lasts 24 hours at 60 °C. The resultant PW@Geopolymers are then sifted and processed with an agate grinder to create a fine powder after the curing process. Before assessing the photodegradation, the PW@Geopolymers are evaluated by several physico-chemical analyses. Geopolymers are nanoscale materials.

Characterization

To determine the chemical constitution of the raw materials Kaolin and PW, the Epsilon 4 X-ray fluorescence spectrometer from Malvern Panalytical was employed. This instrument allowed for the non-destructive analysis of the elemental composition of the samples, providing valuable information about their chemical properties. X-ray analysis (XRD) was performed using a BRUKER D8 ADVANCE diffractometer with a rear monochromator and a copper anti-cathode. This technique enabled the investigation of the crystallographic structure of the samples, shedding light on their phase composition and crystallinity. Microstructural characterization of the precursors and the PW@geopolymers was conducted using an energy dispersive X-ray spectrometer-equipped scanning electron microscopy (SEM), specifically the HIROX SH 4000M model. This combination of SEM and energy-dispersive X-ray spectroscopy (EDX) allowed for the visualization and elemental analysis of the samples at a high magnification, providing valuable insights into their microstructure and chemical composition. For the assessment of MB removal percentage, a HITACHI UV-4100 spectrophotometer was employed to capture the diffuse reflectance UV-Visible spectrum. This technique enabled the quantification of the concentration of methylene blue in the solution before and after treatment, allowing for the calculation of the percentage of MB removal more details for

is presented in the next section. Overall, this research design combined X-ray fluorescence, XRD, SEM-EDX, and UV-Visible spectroscopy to comprehensively analyze the chemical constitution, crystallographic structure, microstructural characteristics, and the efficiency of MB removal in the investigated materials. These data collection procedures and analysis techniques were selected to provide a thorough understanding of the studied phenomena and ensure the replicability of the study.

Photocatalytic degradation of MB dye

In a beaker containing 100 ml of MB dye aqueous solution of 10 mg/L, 0.4 g of photocatalyst was added. To achieve an adsorption/desorption equilibrium, the solution was magnetically stirred and left in the dark for 30 minutes. After that, it was perpendicularly irradiated from top to down by a UV-lamp (ZW-2, 40 W), and centrifuged after every 20 minutes. The absorbance of the supernatant solution was then measured using a UV-Vis spectrophotometer at a maximum absorption wavelength of 660 nm. The following equation (1) was used to compute the deterioration efficiency:

$$i = x = \frac{A_0 - A_t}{A_0} \times 100 \quad (1)$$

Where, μ is the removal efficiency of MB. A_0 and A_t are the absorbency of MB solution at initial time and at time t after UV irradiation at 665 nm, respectively.

Results and Discussion

Material characterization

Table 1 displays the chemical analysis of the MK, which reveals that the principal constituents in our clay are around 53.57% SiO₂, 40.95% Al₂O₃, 2.60% K₂O, and 1.5% Fe₂O₃. The majority of the PW minerals, as shown in table 1, are 44.33% CaO, 9.35% SiO₂, and 20.06% P₂O₅, with a mass loss of 25.43% at 900 °C.

Carbonate, fluorapatite, calcite, dolomite, quartz, and palygorskite were all present in the XRD patterns, as shown in figure 1. A new study conducted by our research team utilizing the same PW [21] supports this. They demonstrated the existence of the pre-sited phases through Rietveld refinement.

The crystallographic structure of MK is shown in figure 1. After being heated, the clay changed from having a more reactive amorphous structure known as MK to a less reactive crystalline structure. This phase is indicated in the XRD analysis by a significant bump between 18 and 35 in the 2-theta position, which distinguished MK from other varieties of kaolin and showed the amorphous structure after calcination and denoted the activation and amorphization of the crystalline phase of the kaolin. It was also observed that the unique quartz

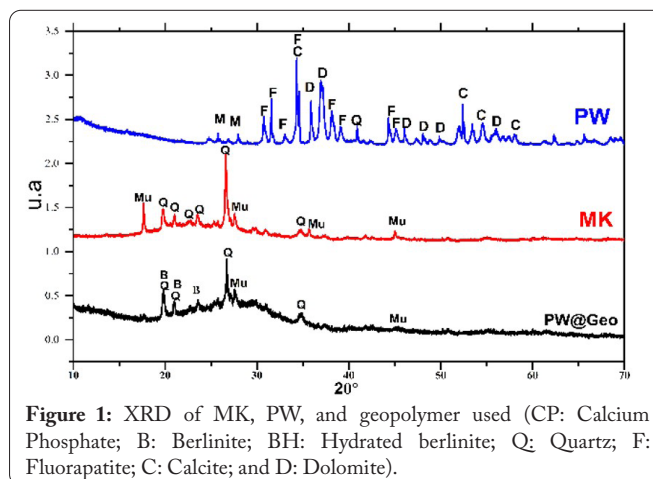


Figure 1: XRD of MK, PW, and geopolymer used (CP: Calcium Phosphate; B: Berlinite; BH: Hydrated berlinite; Q: Quartz; F: Fluorapatite; C: Calcite; and D: Dolomite).

and muscovite peaks were clearer and more pronounced following heat treatment. The XRD data for PW@Geopolymers are shown in figure 1. The crystalline phase of berlinite (aluminum phosphate-AlPO₄) [PDF 10-423] has developed. Quartz (SiO₂) and this new substance, berlinite, are structurally linked, as shown by the XRD [PDF 74-1811] [16]. Small peaks can be detected in quartz [PDF 02-0056] and muscovit [PDF 21-1272]. Since they were already present in raw MK, geopolymerization did not change these crystalline phases.

TGA-DTG analysis was used to characterize the produced geopolymers. The outcomes are shown in figure 2. Due to the absorbed water contained in the geopolymer structure, the PW@Geopolymer exhibits a peak up to 75 °C [33, 34]. The loss of physically absorbed water molecules is what causes the small second breakdown that occurred at 175 °C. According to XRD examination, the weak peaks between 300 and 400 °C are attributed to hydrotalcite, while the peak at 450 °C indicates the existence of chemical water associated with weakly crystalline calcium carbonate phases. Between 600 and 750 °C, there was a noticeable weight loss [34-36]. Dolomite and calcite, which are carbonates from the PW, are fundamentally involved in this.

The SEM is utilized to examine the micromorphology of adsorbent materials. The SEM/EDX micrographs are shown in figure 3. PW@Geopolymer exhibits an amorphous texture, and the formation of crystalline microstructures has been observed, confirming the generation of geopolymers and the reaction between MK, PW, and phosphorus. A porous structure has also been observed, which provides channels for the adsorption of MB and facilitates the adsorption process, followed by photo degradation. The EDX analysis reveals that the precursor used in this study is composed of Si, Al, P, and Ca. Among these major elements, the first three constitute the main components of the geopolymer network, while Ca originates from the PW used. The EDX analysis also indicates the presence of trace amounts of Mg and Fe. These elements

Table 1: Chemical composition of MK and PW.

| Compounds | SiO ₂ | Al ₂ O ₃ | CaO | Fe ₂ O ₃ | K ₂ O | MgO | MnO | Na ₂ O | P ₂ O ₅ | TiO ₂ | LOI |
|-----------|------------------|--------------------------------|-------|--------------------------------|------------------|------|------|-------------------|-------------------------------|------------------|-------|
| MK | 53.57 | 40.95 | - | 1.5 | 2.60 | 0.34 | 0.85 | - | - | 0.07 | 2.72 |
| PW | 9.35 | 4.38 | 44.33 | 2.32 | 0.25 | 3.10 | 1.01 | 0.03 | 20.06 | 0.35 | 25.43 |

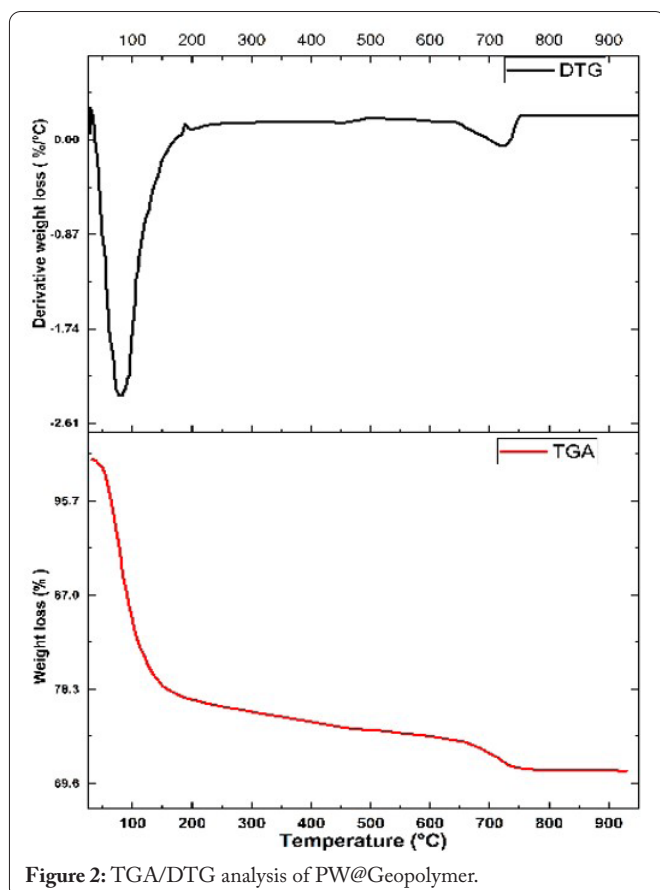


Figure 2: TGA/DTG analysis of PW@Geopolymer.

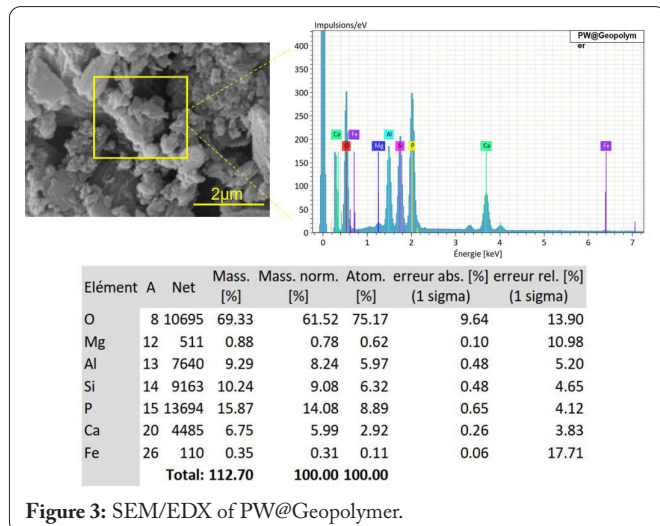


Figure 3: SEM/EDX of PW@Geopolymer.

come from the MK used, and PW is an important element that acts as a semiconductor to catalyze the photodegradation of organic pollutants.

Parametric study

In figure 4, we note that at the beginning, the increase of the pH favors the reaction. Great adsorption of MB in the presence of PW@Geopolymers in basic medium. As MB is a cationic dye, there is a competition between the H⁺ ions contained in the acid and the cationic ions of the dye at the level of the active site of the catalyst, which can explain the greater adsorption of the dye in the basic medium at the first minutes of the reaction. Three experiments were conducted for pho-

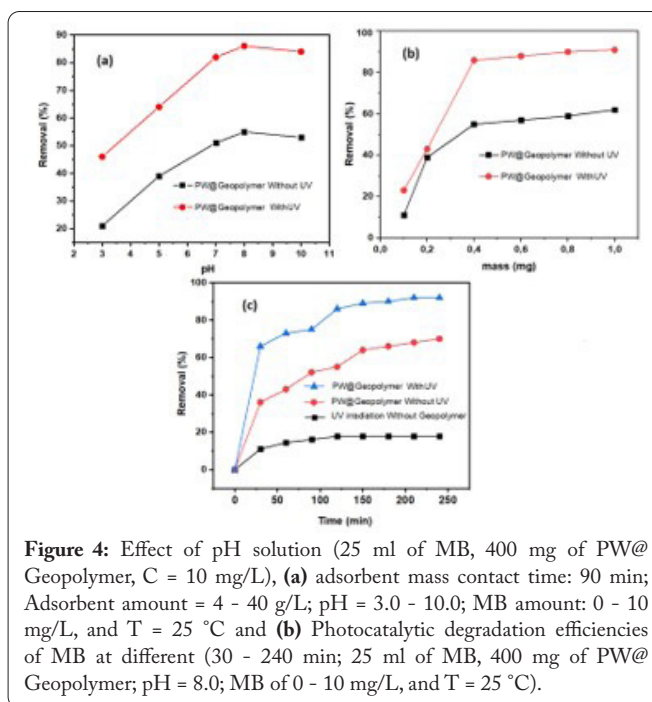


Figure 4: Effect of pH solution (25 ml of MB, 400 mg of PW@Geopolymer, C = 10 mg/L), (a) adsorbent mass contact time: 90 min; Adsorbent amount = 4 - 40 g/L; pH = 3.0 - 10.0; MB amount: 0 - 10 mg/L, and T = 25 °C and (b) Photocatalytic degradation efficiencies of MB at different (30 - 240 min; 25 ml of MB, 400 mg of PW@Geopolymer; pH = 8.0; MB of 0 - 10 mg/L, and T = 25 °C).

tocatalytic MB dye degradation using PW@Geopolymer, as shown in figure 4c. The first explores the efficiency of MB dye degradation by direct photolysis, in which an aqueous solution of MB dye is exposed to UV light without photocatalysis [37, 38]. The second route intends to explore the removal rate of MB by adsorption. The last route attempts to study the rate of photocatalytic degradation of MB, in which an aqueous solution of MB containing the photocatalyst is exposed to UV light. Comparing the results, it is found that the removal efficiency of MB is in the following order: photocatalysis > adsorption > direct photolysis. The lowest photolysis rate of 17.8% in the first pathway indicates that some MB molecules can be directly decomposed by UV light without a catalyst. The highest photocatalytic degradation rate of 91.7% is considered to be the result of a synergistic effect of semiconductor adsorption and photocatalysis. To appreciate the effect of the catalyst amount on the reaction rate, the catalyst dose was doubled from 4 g/L to 40 g/L. By doubling the amount of catalyst, the solution degrades much faster with an abatement rate increasing from 42% to 87%. As previously predicted, the amount of catalyst plays a role in the speed of the reaction by increasing the number of active sites.

Mechanism of MB degradation by PW@Geopolymer photocatalyst

Five stages may be used to explain the photocatalytic reaction process figure 5. Photodegradation is a phenomenon in which a substance undergoes degradation or decomposition upon exposure to light. In the case of the study at hand, the focus is on the photodegradation of MB dye in wastewater using PW@Geopolymer as a photocatalyst. The photodegradation process involves the combined effects of adsorption and photocatalysis. In the initial step, the MB dye molecules in the aqueous solution ionize, forming MB cations. These cations are then adsorbed onto the PW@Geopolymer framework, which contains negatively charged sites, such as the [AlO₄]⁵⁻

tetrahedra. The adsorption process occurs due to electrostatic interactions between the cations and the negatively charged sites [4].

Next, when the PW@Geopolymer is exposed to UV radiation, the metal oxide semiconductor particles, such as Fe_2O_3 , within the PW@Geopolymer become excited. This excitation leads to the generation of electron (e^-) and hole (h^+) pairs [27]. Within the PW@Geopolymer, the generated excited electrons (e^-) interact with the transition metal ions, specifically Fe^{3+} , resulting in the reduction of Fe^{3+} to Fe^{2+} . Simultaneously, the holes (h^+) react with water (H_2O) molecules, leading to the formation of highly reactive hydroxyl radicals ($\bullet OH$) [5]. The $\bullet OH$ play a crucial role in the degradation process. They are strong oxidizing agents that can attack and oxidize the adsorbed MB cations on the PW@Geopolymer surface. This oxidation process breaks down the dye molecules, resulting in the degradation of MB [2, 39]. Overall, the coupled adsorption and photocatalytic processes in PW@Geopolymer contribute to the high degradation efficiency observed in the study. The adsorption of MB cations onto the PW@Geopolymer framework enhances the proximity of the dye molecules to the photocatalytic active sites. Subsequently, under UV radiation, the excited electrons and $\bullet OH$ radicals generated within the PW@Geopolymer initiate oxidation reactions, leading to the degradation of the MB dye molecules. We can summarize the mechanisms of MB removal of this study as follows:

- Step 1: In aqueous solution, the MB molecules ionize to form cations.
- Step 2: MB cations are adsorbed onto the negatively charged $[AlO_4]^{5-}$ tetrahedron present in PW@Geopolymer network.
- Step 3: An excited electron (e^-) and hole (h^+) pairs are created when the metal oxide semiconductor particles,

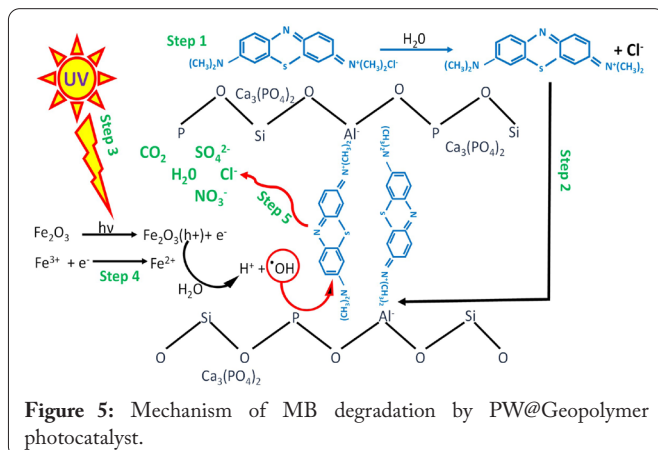


Figure 5: Mechanism of MB degradation by PW@Geopolymer photocatalyst.

such as Fe_2O_3 (4.78 wt.%), contained in the PW@Geopolymer, are exposed to UV radiation.

- Step 4: The transition metal ions of Fe^{3+} present in the PW@Geopolymer interact with the electron (e^-) to form Fe^{2+} . and the $\bullet OH$ radical is created when the hole (h^+) and H_2O molecules interact.
- Step 5: $\bullet OH$ radicals oxidize the MB cations adsorbed on the PW@Geopolymer framework to produce the degradation products.

Photocatalysis and adsorption kinetics

MB absorption kinetic data were simulated using pseudo-first order and pseudo-second order models to understand the chemical nature of the absorption process [13]. These models are structured as follows:

$$\frac{t}{\left[\frac{1}{k_2 Q_e^2} \right] + \left[\frac{1}{Q_e} \right] t} \quad (2)$$

$$Q_t = Q_e (1 - e^{-k_1 t}) \quad (3)$$

Where, Q_e (mg/g) refers to the amount adsorbed at equilibrium, Q_t (mg/g) represents the amount adsorbed at time t.

The parameters k_1 (min^{-1}) and k_2 ($mg^{-1}min^{-1}$) are the adsorption rate constants of models pseudo-first and pseudo-second, respectively. The adsorbed quantities Q_t , pseudo-second order constants k_2 and regression coefficients R^2 for the concentrations used are given in table 2. The equilibrium adsorption capacity (Q_e) as well as the correlation coefficients (R^2) of the lines are presented in table 1, which shows the correlation coefficients ($R^2 \geq 0.99$) of the lines plotted by plotting qt versus t (Figure 6) and shows small deviations between the experimental Q_e and calculated Q_e (Table 2), indicating that the pseudo-second order kinetic model can be applied to MB removal by using PW@Geopolymers.

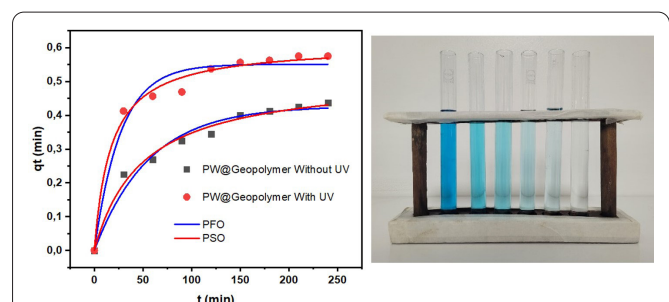


Figure 6: Pseudo-first order and pseudo-second order model for of MB on PW@Geopolymer (Experiment conditions: 25 ml of MB, 400 mg of PW@Geopolymer, and C = 10 mg/L).

Table 2: Kinetics adsorption parameters of MB on PW@Geopolymer.

| | qe,exp (mg/g) | Pseudo-first order model | | | Pseudo-second order model | | |
|-----------------|---------------|--------------------------|------------|----------------|---------------------------|---------------|----------------|
| | | qe,cal (mg/g) | K1 (1/min) | R ² | qe,cal (mg/g) | K2 (g/mg.min) | R ² |
| PW@G without UV | 0.473 | 0.427 | 0.018 | 0.967 | 0.518 | 0.039 | 0.992 |
| PW@G with UV | 0.589 | 0.550 | 0.037 | 0.969 | 0.609 | 0.094 | 0.995 |

Isotherms adsorption

The sorption isotherms of MB on PW@Geopolymers have been described with the widely used Langmuir and Freundlich models (Figure 7). Both models are given by the following equations 4 and 5 [3, 4].

$$Q_e = \frac{K_L q_m C_e}{1 + K_L C_e} \quad (4)$$

$$Q = K_f C_e^n \quad (5)$$

Where, q_e (mg/g) is the adsorbed amount, q_m (mg/g) represents the maximum surface coverage, K_L (L/mg) is the Langmuir constant associated with the binding capacity and C_e (mg/L) denotes the equilibrium solution concentration, and K_f stands for the Freundlich constant associated with the absorption capacity, while n is the linearity constant.

The values of the regression coefficients obtained indicate that the adsorption process of MB on PW@Geopolymer is described in a favorable way by the Langmuir isotherm (with excellent linear regression coefficients R^2 that are very close to unity).

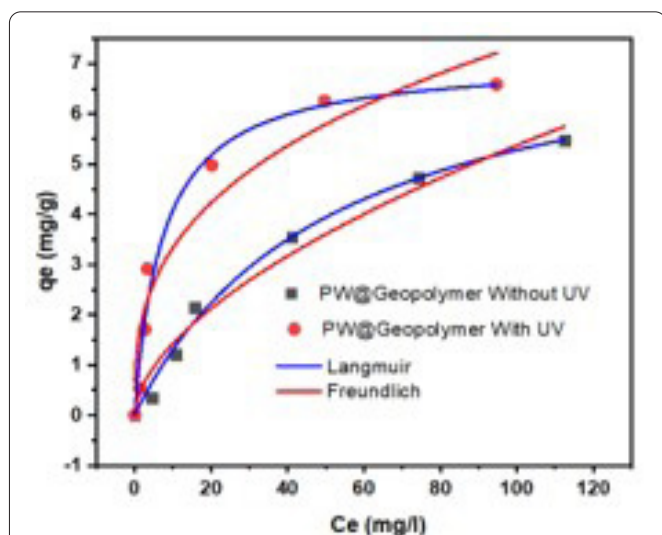


Figure 7: Nonlinear representation of Langmuir isotherm and Freundlich isotherm of MB on PW@Geopolymer (Experiment conditions: 25 ml of MB, 400 mg of PW@Geopolymer, and $C = 10 - 200$ mg/L).

Challenges and Future Study

This study serves as a foundational exploration of the potential application of PW@Geopolymer as a photocatalyst for dye degradation. However, it is important to acknowledge that there are several limitations that should be taken into consideration, highlighting the need for further research in this area. Firstly, the generalizability of the findings to other types of geopolymers, different dyes, and alternative irradiation conditions may be limited. Therefore, additional research is required to investigate the applicability of PW@Geopolymer as a photocatalyst across a broader range of materials and conditions. Secondly, the study lacks specific details regarding the synthesis conditions and parameters employed, which introduces the possibility of variations in the properties and

performance of the geopolymers. Understanding the influence of synthesis conditions is crucial for achieving reproducibility and optimizing the photocatalytic properties of PW@Geopolymer. Furthermore, different sources of PW may exhibit variations in their chemical compositions, potentially impacting the photocatalytic performance. It is essential to consider this variability when evaluating the effectiveness of PW@Geopolymer as a photocatalyst. In addition, the study primarily focused on the initial pH and pollutant concentration as governing parameters, while other influential factors such as temperature, light intensity, and the presence of co-existing pollutants were not accounted for. Future studies should incorporate these variables to obtain a more comprehensive understanding of the degradation process. Lastly, the long-term stability and durability of PW@Geopolymer as a photocatalyst were not assessed in this study. Evaluating its performance over extended periods and considering potential degradation or loss of activity is crucial for practical applications. To address these limitations, further research should be conducted using comprehensive experimental designs and rigorous controls. This approach will enhance the validity and reliability of the findings, allowing for a more robust understanding of the potential application of PW@Geopolymer as a photocatalyst for dye degradation.

Table 3: Equilibrium adsorption parameters of MB on PW@Geopolymer.

| | Langmuir | | | Freundlich | | |
|-----------------|-------------|------------|-------|------------|------|-------|
| | qmax (mg/g) | KL (L/min) | R2 | KF (mg/g) | n | R2 |
| PW@G without UV | 7.09 | 0.991 | 0.991 | 0.41 | 0.34 | 0.951 |
| PW@G with UV | 8.01 | 0.995 | 0.997 | 1.54 | 0.57 | 0.895 |

Conclusion

Geopolymers made of phosphoric acid and PW were utilized for the first time as novel photocatalysts in the current study to evaluate the photodegradation of the wastewater dye MB. The starting pH of the solution and the concentration of the pollutant are the physico-chemical factors that were investigated, and which control the kinetics. Due to the cooperative action of adsorption and semiconducting photocatalysis, the degradation efficiency of the MB dye by PW@Geopolymer was up to 91.7% when exposed to UV light. The examination of the MB dye's adsorption kinetics was correlated using the pseudo-first and pseudo-second order speed equations. Both with and without UV irradiation, the experimental results, and the equation for the pseudo-second order rate agreed well. Third order reaction kinetics govern the photocatalytic breakdown of the MB dye in solution.

Acknowledgements

None.

Conflict of Interest

None.

References

1. Billah RE, Islam MA, Lgaz H, Lima EC, Abdellaoui Y, et al. 2022. Shellfish waste-derived mesoporous chitosan for impressive removal of arsenic (V) from aqueous solutions: a combined experimental and computational approach. *Arab J Chem* 15(10): 104123. <https://doi.org/10.1016/j.arabjc.2022.104123>
2. Ammari Y, Elatmani K, Qourzal S, Bakas I, Ejakouk E, et al. 2016. Kinetic study of the photocatalytic degradation of methylene blue dye in the presence of titanium dioxide (TiO₂), in aqueous suspension. *J Mater Environ Sci* 7(8): 671-678.
3. Billah RE, Shekhawat A, Mansouri S, Majdoubi H, Agunaou M, et al. 2022. Adsorptive removal of Cr (VI) by chitosan-SiO₂-TiO₂ nanocomposite. *Environ Nanotechnol Monit Manag* 18: 100695. <https://doi.org/10.1016/j.enmm.2022.100695>
4. Khan MI, Min TK, Azizli K, Sufian S, Ullah H, et al. 2015. Effective removal of methylene blue from water using phosphoric acid based geopolymers: synthesis, characterizations and adsorption studies. *RSC Adv* 5(75): 61410-61420. <https://doi.org/10.1039/c5ra08255b>
5. Zhang Y, Liu L. 2013. Fly ash-based geopolymer as a novel photocatalyst for degradation of dye from wastewater. *Particuology* 11(3): 353-358. <https://doi.org/10.1016/j.partic.2012.10.007>
6. Oubakalla M, Beraich M, Taibi M, Majdoubi H, Aichi Y, et al. 2022. The choice of the copper concentration favoring the production of stoichiometric CuSbS₂ and Cu₂Sb₄S₁₃ thin films co-electrodeposited on FTO. *J Alloys Compd* 908: 164618. <https://doi.org/10.1016/j.jallcom.2022.164618>
7. Billah RE, Khan MA, Wabaidur SM, Jeon BH, Am A, et al. 2021. Chitosan/phosphate rock-derived natural polymeric composite to sequester divalent copper ions from water. *Nanomaterials* 11(8): 2028. <https://doi.org/10.3390/nano11082028>
8. Allaoui D, Nadi M, Hattani F, Majdoubi H, Haddaji Y, et al. 2022. Eco-friendly geopolymer concrete based on metakaolin and ceramics sanitaryware wastes. *Ceram Int* 48(23): 34793-34802. <https://doi.org/10.1016/j.ceramint.2022.08.068>
9. Haddaji Y, Majdoubi H, Mansouri S, Tamraoui Y, Manoun B, et al. 2021. Effect of synthetic fibers on the properties of geopolymers based on non-heat treated phosphate mine tailing. *Mater Chem Phys* 260: 124147. <https://doi.org/10.1016/j.matchemphys.2020.124147>
10. Majdoubi H, Haddaji Y, Mansouri S, Alaoui D, Tamraoui Y, et al. 2021. Thermal, mechanical and microstructural properties of acidic geopolymer based on moroccan kaolinitic clay. *J Build Eng* 35: 102078. <https://doi.org/10.1016/j.jobte.2020.102078>
11. Billah RE, Khan MA, Park YK, Am A, Majdoubi H, et al. 2021. A comparative study on hexavalent chromium adsorption onto chitosan and chitosan-based composites. *Polymers* 13(19): 3427. <https://doi.org/10.3390/polym13193427>
12. Beraich M, Shaili H, Hafidi Z, Benhsina E, Majdoubi H, et al. 2020. Facile synthesis of the wurtz stannite (orthorhombic) Cu₂MnGeS₄ thin film via spray ultrasonic method: structural, Raman, optical and electronic study. *J Alloys Compd* 845: 156216. <https://doi.org/10.1016/j.jallcom.2020.156216>
13. Billah RE, El Bachraoui F, El Ibrahimy B, Oualid HA, Kassab Z, et al. 2022. Mechanistic understanding of nickel (II) adsorption onto fluorapatite-based natural phosphate via Rietveld refinement combined with Monte Carlo simulations. *J Solid State Chem* 310: 123023. <https://doi.org/10.1016/j.jssc.2022.123023>
14. Oubakalla M, Beraich M, Taibi M, Majdoubi H, Guenbour A, et al. 2022. Effects of copper concentration on the properties of Cu₂CoSnS₄ thin films co-electrodeposited on the FTO substrate. *J Mater Sci Mater Electron* 33(15): 12016-12025. <https://doi.org/10.1007/s10854-022-08162-4>
15. Majdoubi H, Alqadami AA, Billah RE, Otero M, Jeon BH, et al. 2023. Chitin-based magnesium oxide biocomposite for the removal of methyl orange from water. *Int J Environ Res Public Health* 20(1): 831. <https://doi.org/10.3390/ijerph20010831>
16. Bourzik O, Akkouri N, Baba K, Haddaji Y, Nounah A, et al. 2022. Study of the effects of drinking water treatment sludge on the properties of Class F fly ash-based geopolymer. *Environ Sci Pollut Res* 29(58): 87668-87679. <https://doi.org/10.1007/s11356-022-21873-9>
17. Haddaji Y, Majdoubi H, Mansouri S, Tamraoui Y, Boulif R, et al. 2021. Effect of sodium hexafluorosilicate addition on the properties of metakaolin based geopolymers cured at ambient temperature. *Silicon* 13(5): 1441-1451. <https://doi.org/10.1007/s12633-020-00536-9>
18. Aziz A, Stocker O, El Hassani IE, Laborier AP, Jacotot E, et al. 2021. Effect of blast-furnace slag on physicochemical properties of poz-zolan-based geopolymers. *Mater Chem Phys* 258: 123880. <https://doi.org/10.1016/j.matchemphys.2020.123880>
19. Haddaji Y, Majdoubi H, Mansouri S, Alomayri TS, Allaoui D, et al. 2022. Microstructure and flexural performances of glass fibers reinforced phosphate sludge based geopolymers at elevated temperatures. *Case Studies Constr Mater* 16: e00928. <https://doi.org/10.1016/j.cscm.2022.e00928>
20. Aziz A, El Amrani IE. 2019. Élaboration et caractérisation des géopolymères à base de pouzzolane. Éditions universitaires européennes.
21. Haddaji Y, Hamdane H, Majdoubi H, Mansouri S, Allaoui D, et al. 2021. Eco-friendly geopolymer composite based on non-heat-treated phosphate sludge reinforced with polypropylene fibers. *Silicon* 13: 2389-2400. <https://doi.org/10.1007/s12633-020-00873-9>
22. Becker P. 1989. Phosphates and Phosphoric Acid: Raw Materials, Technology, and Economics of the Wet Process. Revised and expanded. Marcel Dekker, Inc., New York.
23. Oubakalla M, Beraich M, Taibi M, Majdoubi H, Guenbour A, et al. 2022. Effects of co-electrodeposition potential on the physicochemical properties of Cu₂CoSnS₄ thin films enriched by a theoretical calculation. *Optik* 258: 168886. <https://doi.org/10.1016/j.ijleo.2022.168886>
24. Bourzik O, Akkouri N, Baba K, Nounah A. 2022. Study of the effect of wood waste powder on the properties of concrete. *Mater Today Proc* 58: 1459-1463. <https://doi.org/10.1016/j.matpr.2022.02.518>
25. Bourzik O, Baba K, Akkouri N, Nounah A. 2023. Effect of waste marble powder on the properties of concrete. *Mater Today Proc* 72: 3265-3269. <https://doi.org/10.1016/j.matpr.2022.07.184>
26. Akkouri N, Bourzik O, Baba K, Nounah A. 2022. Experimental study of the thermal and mechanical properties of concrete incorporating recycled polyethylene. *Mater Today Proc* 58: 1525-1529. <https://doi.org/10.1016/j.matpr.2022.03.293>
27. Lin WY, Wei C, Rajeshwar K. 1993. Photocatalytic reduction and immobilization of hexavalent chromium at titanium dioxide in aqueous basic media. *J Electrochem Soc* 140(9): 2477. <https://doi.org/10.1149/1.2220847>
28. Akkouri N, Bourzik O, Baba K, Tayeh B. 2021. Mechanical and thermal performances of eco-friendly mortar containing recycled PET as partial sand replacement. *Preprint Research Square*. <https://doi.org/10.21203/rs.3.rs-932046/v1>
29. Sbi S, Aboulayt A, Borja W, Mansouri S, El Idrissi HE, et al. 2022. An advance understanding of the alkali activation of cover layers waste rocks from phosphate mines: mechanical, structure and microstructure studies. *Constr Build Mater* 346: 128472. <https://doi.org/10.1016/j.conbuildmat.2022.128472>
30. Baccour H, Koubaa H, Baklouti S. 2018. Phosphate sludge from Tunisian phosphate mines: valorisation as ceramics products. In *Recent Advances in Environmental Science from the Euro-Mediterranean and Surrounding Regions: Proceedings of Euro-Mediterranean Conference for Environmental Integration, Tunisia*.
31. Majdoubi H, Makhlof R, Haddaji Y, Nadi M, Mansouri S, et al. 2023. Valorization of phosphogypsum waste through acid geopolymer technology: synthesis, characterization, and environmental assessment. *Constr Build Mater* 371: 130710. <https://doi.org/10.1016/j.conbuildmat.2023.130710>

32. Tchakouté HK, Rüscher CH, Kamseu E, Andreola F, Leonelli C. 2017. Influence of the molar concentration of phosphoric acid solution on the properties of metakaolin-phosphate-based geopolymer cements. *Appl Clay Sci* 147: 184-194. <https://doi.org/10.1016/j.clay.2017.07.036>
33. Lemougna PN, Wang KT, Tang Q, Kamseu E, Billong N, et al. 2017. Effect of slag and calcium carbonate addition on the development of geopolymer from indurated laterite. *Appl Clay Sci* 148: 109-117. <https://doi.org/10.1016/j.clay.2017.08.015>
34. Akkouri N, Baba K, Simou S, Alanssari N, Nounah A. 2020. The Impact of Recycled Plastic Waste in Morocco on Bitumen Physical and Rheological Properties. In Ameen H, Jamiolkowski M, Manassero M, Shehata H (eds) *Recent Thoughts in Geoenvironmental Engineering. Sustainable Civil Infrastructures*. Springer, Cham, pp 131-145.
35. Cwirzen A, Provis JL, Penttala V, Habermehl-Cwirzen K. 2014. The effect of limestone on sodium hydroxide-activated metakaolin-based geopolymers. *Constr Build Mater* 66: 53-62. <https://doi.org/10.1016/j.conbuildmat.2014.05.022>
36. Akkouri N, Baba K, Simou S, ELfarissi L, Nounah A. 2020. Recycled thermoplastics modified bitumen improved with thermoplastic elastomer. *E3S Web Conf* 150: 02015. <https://doi.org/10.1051/e3s-conf/202015002015>
37. Billah RE, Kaya S, Şimşek S, Halim EM, Agunaou M, et al. 2023. Removal and regeneration of As (V) in aqueous solutions by adsorption on calcined fluorapatite. *Int J Environ Sci Technol* 20(5): 5197-5206. <https://doi.org/10.1007/s13762-022-04459-3>
38. Akkouri N, Baba K, Elkassia AA. 2023. Valorization of plastic waste (PP-LDPE) from Moroccan industry in modification of hybrid bitumen: application of the mixture design methodology. *Int J Pavement Technol* 16(3): 760-779. <https://doi.org/10.1007/s42947-022-00162-1>
39. Ettahiri Y, Bouargane B, Fritah K, Akhsassi B, Pérez-Villarejo L, et al. 2023. A state-of-the-art review of recent advances in porous geopolymer: applications in adsorption of inorganic and organic contaminants in water. *Constr Build Mater* 395: 132269. <https://doi.org/10.1016/j.conbuildmat.2023.132269>